"Design, Spectroscopic Characterization, DNA Binding, and Biological Activity of Zn (II) Complexes of 6-Aminobenzothiazole-Based Schiff Bases"

K. Jagadesh babu[1]*, Dr. SatyanarayanaKandala[2], Koyada Vivek[3]

[1]Department of Chemistry, Government Degree College, Parkal, Hanamkonda, Telangana-506164, India

[2]DepartmentofChemistry, Government Degree college, (A), Narsampet, Telangana-506132, India

[3]SRM Institute of Science and Technology, Trichy, Tamil Nadu - 621 105, India

DOI: https://doi.org/10.51584/IJRIAS.2026.11090189

Received: 05 October 2026; Accepted: 10 October 2026; Published: 28 October 2026

ABSTRACT

Two novel Zn(II) complexes derived from 6-aminobenzothiazole-based Schiff base ligands (HL1 and HL2) were synthesized and comprehensively characterized using spectroscopic and analytical techniques, including mass spectrometry, FT-IR, UV–Vis spectroscopy, magnetic susceptibility, and thermogravimetric analysis (TGA). The complexes, formulated as $[Zn(HL)_2(H_2O)_2]$, were found to exhibit a six-coordinate octahedral geometry. DNA-binding studies, carried out using electronic absorption and fluorescence spectroscopy, indicated an intercalative mode of interaction, with binding affinities following the order 2a > 1a. The complexes also demonstrated efficient DNA cleavage activity under oxidative and photolytic conditions, showing greater efficacy than the free ligands. In vitro cytotoxicity studies against A549 (lung cancer) and MCF-7 (breast cancer) cell lines revealed enhanced anticancer activity for the Zn(II) complexes. Furthermore, antimicrobial investigations confirmed that the metal complexes possess superior activity compared to their parent ligands. Overall, the results suggest that the synthesized Zn(II) complexes are promising candidates for potential therapeutic applications.

INTRODUCTION

Coordination compounds have emerged as a significant class of materials in medicinal chemistry due to their diverse therapeutic and diagnostic potential. The unique electronic configurations of transition metal ions enable precise modulation of molecular properties that are often unattainable with purely organic frameworks [1]. The biological activity of metal complexes is largely dictated by their coordination geometry, reactivity, and physicochemical characteristics, making ligand design a critical factor in enhancing their efficacy [2]. In this regard, multidentate ligands with suitable donor atoms play a pivotal role in constructing biologically active metal complexes.

Among these, Schiff bases (imines), obtained via the condensation of primary amines with aldehydes or ketones, represent an important class of ligands owing to their synthetic simplicity, structural diversity, and strong coordination ability through nitrogen and oxygen donor sites [3,4]. Their metal complexes have attracted considerable attention because of their wide-ranging biological activities, including antimicrobial, anticancer, antioxidant, and antiviral properties [5–6]. Notably, the interaction of metal complexes with DNA has been recognized as a key mechanism underlying their anticancer activity, as such interactions can disrupt DNA replication and transcription, ultimately leading to apoptosis [7]. These interactions are commonly investigated using techniques such as electronic absorption spectroscopy, fluorescence quenching, viscosity analysis, and gel electrophoresis [10]. In addition to anticancer applications, transition metal complexes have also shown promise in the management of metabolic disorders such as diabetes mellitus (DM), a condition characterized by chronic hyperglycemia and associated complications including neuropathy, nephropathy, and retinopathy. Inhibition of carbohydrate-metabolizing enzymes such as α-amylase by metal complexes offers a potential therapeutic

strategy [9, 10]. Furthermore, their ability to alleviate oxidative stress through enhanced antioxidant activity adds to their pharmacological relevance.

Chelation of Schiff base ligands with biologically important metal ions such as Cu^{2+}, Co^{2+}, Ni^{2+}, Mn^{2+}, Fe^{2+}, and Zn^{2+}, has been shown to enhance biological activity by increasing lipophilicity and reducing polarity, thereby improving cellular uptake [11]. Although platinum-based drugs such as cisplatin remain widely used in chemotherapy, their clinical utility is limited by severe side effects and the development of drug resistance, necessitating the development of safer and more selective alternatives [12].

In this context, the present study focuses on the synthesis, characterization, and biological evaluation of novel Zn(II) complexes derived from Schiff base ligands obtained by the condensation of 6-aminobenzothiazole with 3,5-dichlorosalicylaldehyde and 3-bromo-5-chlorosalicylaldehyde. Particular attention has been given to their thermal stability, antibacterial activity, cytotoxic potential, and DNA-binding interactions as a possible mechanism of action.

MATERIAL AND METHODS

Materials

All of the preparatory materials and solvents were procured from Sigma-Aldrich, Merck, and Hi Media Ltd. The solvents used for the synthesis were thoroughly distilled and dried according to standard methods. The Supercoiled pBR322 DNA and CT-DNA were purchased from Genei in Bangalore, India, and kept at 4 ºC. Double-distributed water was used to prepare all of the buffer solutions for the DNA binding and cleavage experiments.

Methods

The elemental analysis (C, H, N and S) of all the synthesised compounds was performed using a Perkin-Elmer elemental analyzer. FT-IR spectra were recorded on the Perkin-Elmer Infrared Model 337 in the range 4000-250 cm^{-1}. UV-Vis spectra of compounds were analysed on a Shimadzu UV-Vis 2600 spectrophotometer in DMSO solvent in the range between 200 and 800 nm. ESI mass spectra were recorded on an HP-LC mass spectrometer (Agilent Tech, USA). The metal content of the complexes was determined using atomic absorption spectroscopy with the GBC Avanta 1.0 AAS. The melting points of the compounds were determined on a Polmon instrument (model No.MP-96. The thermo gravimetric analysis (TGA) of all metal complexes were carried out in a dynamic nitrogen atmosphere with a heating rate of 10 ºC min^{-1} on a Shimadzu TGA-50H in the temperature range of 27–1200 ºC. Fluorescence spectra were recorded on a Shimadzu RF-5301PC spectrofluorometer.

Synthesis of Schiff base Ligansds (HL_1 and HL_2):

The ligands **HL_1** and **HL_2** were synthesized according to a previously reported procedure [13]. A hot methanolic solution of 6-aminobenzothiazole (10 mM) was magnetically stirred in a round-bottom flask. To this, an equimolar methanolic solution (10 mM) of either 3,5-dichlorosalicylaldehyde or 3-bromo-5-chlorosalicylaldehyde was added dropwise under continuous stirring. The reaction mixture was refluxed at 70–80 °C for 5 hours, and the progress of the reaction was monitored by thin-layer chromatography (TLC). Upon completion, the resulting solid product was isolated by filtration, washed thoroughly with petroleum ether followed by methanol, and dried in a vacuum desiccator over anhydrous $CaCl_2$ to obtain the corresponding Schiff bases. The synthetic route is illustrated in **Scheme 1**.

benzo[d]thiazol-6-ylimino)methyl)-4,6-dichlorophenol

($C_{14}H_8Cl_2N_2OS$), (HL_1):

Yield:76%. M.P: 135 ºC. Elamental Analysis. Calcd (%):Molecular formula $C_{14}H_8Cl_2N_2OS$; Calculated: C, 52.03; H, 2.49; N, 8.67; S, 9.92. Found: C, 52.11; H, 2.52; N, 8.72; S, 9.98; **Melting Point:** 175 ºC.. IR (KBr): $\nu_{(O-H)}$ 3460, $\nu_{(CH=N)}$ 1622, $\nu_{(C-O)}$ 1174 (Fig. S1). UV-Vis; lmax/nm (cm-1): 260 (38461), 318 (31446), (Fig.S2). ^{1}H NMR (400 MHz, CDCl3) δ: **):** 14.02 (s, 1H); 9.03 (s, 1H); 8.66 (s, 1H); 8.19 (d, 1H); 7.88 (d, 1H); 7.50-7.48

(m, 2H); 7.34 (d, 1H) (Fig. S3). ^{13}C NMR (100 MHz, CDCl3) (δ); 161.0, 155.8, 154.8, 152.8, 144.7, 135.1, 133.0, 129.9, 124.5, 123.6, 122.9, 120.2, 119.9, 114.6 (Fig. S4). LC-MS (m/z): Calc: 309.17: Found: 321 (M-2).

benzo[d]thiazol-6-ylimino)methyl)-6-bromo-4-chlorophenol ($C_{14}H_8BrClN_2OS$), (HL_2)

Yield: 75%; M.p: 138 °C; Anal. Calc (%):C, 45.74; H, 2.19; N, 7.62; S, 8.72. Found: C, 45.81; H, 2.23; N, 7.79; S, 8.89;**Melting Point:**180 ºC.. IR (KBr): $\nu_{(O-H)}$ 3467, $\nu_{(CH=N)}$ 1622, $\nu_{(C-O)}$ 1152, (Fig. S1). UV-Vis: lmax/nm (cm-1); 258 (38759), 334 (29940), (Fig-S2). ^{1}H NMR (400 MHz, CDCl3): δ; 14.17 (s, 1H); 9.04 (s, 1H); 8.64 (s, 1H); 8.19 (d, 1H); 7.89 (d, 1H); 7.66 (d, 1H); 7.49 (d, 1H); 7.39 (d, 1H), (Fig. S3). ^{13}C NMR (100 MHz, CDCl3): δ; 160.9, 156.6, 154.9, 152.8, 144.6, 135.8, 135.1, 130.6, 124.5, 124.0, 120.1, 120.0, 114.6, 111.8, (Fig. S4). ESI–MS (m/z):Calc: 369(M+2).

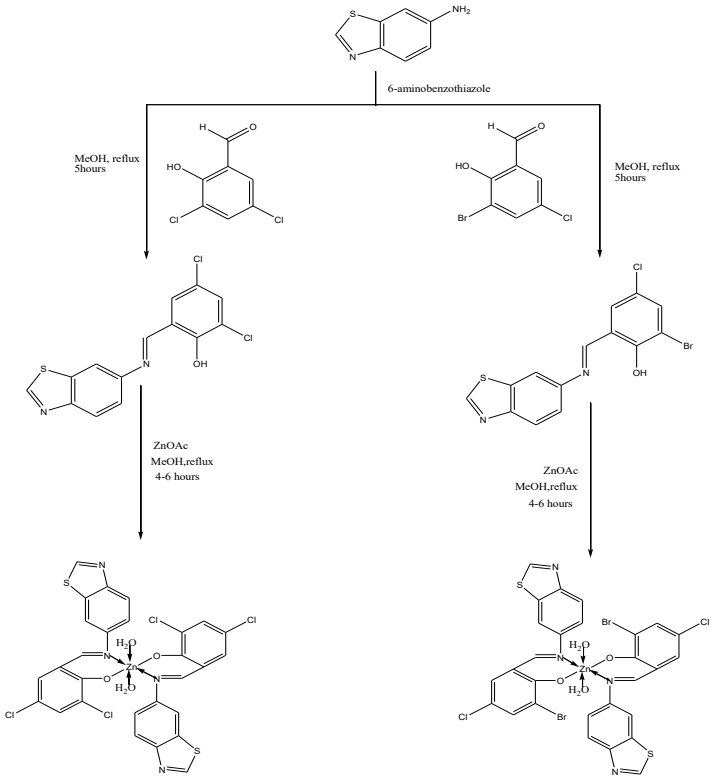

Scheme 1. Synthesis of Schiff base and corresponding 1a and 2a complexes.

Synthesis of binary metal complexes (1a-2a):

The Zink metal complexes **1a** and **2a** were synthesized reacting the Schiff base ligands with the corresponding metal salts in a 1:2 (metal:ligand) molar ratio. A hot methanolic solution (10 mM) of $Zncl_2$ was added dropwise to a hot, magnetically stirred methanolic solution of the Schiff base ligands (HL_1/HL_2) (20 mM). The reaction mixture was refluxed at 70–80 °C for 4–6 h with continuous stirring, and the progress of complex formation was monitored periodically. Upon completion, the resulting colored solid complexes were isolated by filtration, washed successively with hot methanol and petroleum ether to remove unreacted materials and impurities, and then dried in a vacuum desiccator over anhydrous $CaCl_2$. The general synthetic route for the ligands and their corresponding metal complexes (1a and 2a) is illustrated in **Scheme 1**.

$[Zn(HL_1)_2(H_2O)_2]$: ($C_{28}H_{18}Cl_4N_4O_4S_2Zn$) (1a):

Color: light orange Yield: 79%, M.pt: ~125 ºC, Anal. Found. (Cal.) C, 45.02(45.09); H, 2.13 (2.43); Zn, 8.60 (8.77); N, 7.23 (7.51); S, 8.45 (8.60); IR (KBr) (cm-1): ν(O-H) 3426: ν(HC=N) 1622, ν(C–O) 1166, ν(M–O) 521, ν(M–N) 436;; UV-Vis (DMSO) λmax/nm (cm-1): 265 (37736), 331 (30211), 421 (23753); μeff (BM): 0; MS (ESI): m/z 747.7 $[M+2]^+$ (**Fig.S3.1a**).

$[Zn(HL_2)_2(H_2O)_2]$: ($C_{28}H_{18}Br_2Cl_2N_4O_4S_2Zn$) (2a):

Color: yellowish orange, Yield: 75%, M.pt: ~129 ^oC, Anal. Found. (Cal.) C, 41.02(40.29); H, 2.08 (2.17); Zn, 7.60 (7.83); N, 6.53 (6.71);S, 7.52 (7,68); IR (KBr) (cm^{-1}): ν(O-H) 3452: ν(HC=N) 1618, ν(C–O) 1146, ν(M–O) 545, ν(M–N) 465; UV-Vis (DMSO) λmax/nm (cm^{-1}): 254 (39370), 330 (30303), 430 (23255); μeff (BM): 0; MS (ESI): m/z 836.7 $[M+2]^+$ (**Fig.S3.2a**).

DNA binding studies:

UV–Vis spectroscopic studies:

The DNA binding affinities of three monometallic complexes (1a, 1b and 1c) were assessed using the UV-visible absorption method. The complex concentration maintained constant of 10μM, while the concentration of CT-DNA varied from 0 to 10 μM. The complexes were initially dissolved in DMSO due to limited solubility in buffer solution. To prepare the CT-DNA stock solution, DNA was diluted in a Tris-HCl/NaCl buffer at pH = 7.2 (50mM NaCl/5 mM Tris-HCl). The purity of the CT-DNA was ensured by measuring UV spectra using molar extinction coefficient of 6600 M^{-1} at 260 nm [13]. Mixing the CT-DNA solution with the respective complex and reference solution, followed by five minutes incubation before recording the absorption spectra. By analyzing the absorption data we determined the intrinsic binding constant (K_b) for interaction of each complex with CT-DNA.

Fluorescence quenching study:

Using fluorescence spectrophotometer and EB-bound CT-DNA in Tris HCl/NaCl buffer (pH 7.2), the binding between metal complexes and CT-DNA was investigated. The emission spectra of CT-DNA (125 μM) bound to EB (12.5 μM) were captured in the 360–800 nm region (350 nm excitation) as complex quantities were varied from 0 to 60 μM. The comparative binding affinity of the complexes with CT-DNA was calculated using the quenching constant derived by the Stern-Volmer equation [14], Io/I = 1 + Ksv r. The fluorescence (emission band) intensities in the absence and presence of complexes are denoted by I_o and I, respectively; K_{sv} is a linear Stern-Volmer constant; and 'r' is the complex concentration as a proportion of the DNA concentration.

DNA cleavage:

The ability of schiff base and its monometallic metal compounds (1a, 1b and 1c) to cleave DNA was evaluated using agarosegel electrophoresis in the presence and absence of H_2O_2. Super coiled pBR322 DNA was diluted in a Tris-HCl/NaCl buffer at pH 7.2, and treated with varying concentrations of the metal complexes [15]. After a two hour incubation at room temperature, bromophenol blue (2μL) was added to the DNA sample followed by vigorous stirring. The sample was then loaded onto a 1% agarosegel containing a TAE buffer (PH 8.0) and subjected to electrophoresis at 70 V for 45 minutes. Prior to electrophoreses, the gel was stained with ethidiumbromide. The resulting gel is photographed using the BIO-RAD Gel documentation system, and the DNA bands were observed under transilluminators.

Biological Evaluation:

Anti bacterial activity:

In vitro testing was using the agar well diffusion metbod to evaluate the antibacterial activity of all synthesized compounds (HL, 1a, 1b and 1c) and the standard drug Gentamycin sulphate against two Gram positive (Staphylococcus aureus and Bacillus subtilis) and two Gram negative (Escherichia coli and Klebsiella pneumonia) bacterial stains. The bacterial culture was deposited on medium dishes after 24 hours of growth. Wells with three different concentrations (25, 50 75, μg/well) were created using a 6 mm cork borer. The plates were incubated at 25 ± 2°C and inhibition zones were measured in mm and compared with the standard drug zones.

Anti fungal activity:

Agarwell diffusion method was used to check in vitro anti fungal activity of synthesized compounds against two fungi species are Aspergillus niger and Candida albicans. One week old fungal culture was used as inoculums. Nystatin was used as reference antifungal drug. Antifungal data of compounds were expressed from the area of their inhibitory zone.

Anticancer activity (MTT assay):

Synthesized substances (HL_1, HL_2, 1a, and 2a) were tested for their cytotoxicity on A-549 and MCF-7 cell lines. Cell viability was determined using the MTT assay. Tumour cells were cultured in 25 cm^2 flasks with appropriate medium at 37 °C in a CO_2 incubator. MCF-7 and A-549 cells were separately plated in a 96-well plate. After overnight growth, the cells were switched to low serum media. DMSO was used as the control. After 48 hours of exposure to different synthesized substances, the cells were treated with MTT solution for 4 hours. Then, the medium was removed. Optical density at 570 nm was measured using an ELISA plate reader, representing cell quantity. The results were reported as a percentage of cytotoxicity/viability. Every experiment was taken in triplicates, and the cytotoxicity of the test substance Doxorubicin was compared to determine the IC_{50} values.

RESULTS AND DISCUSSION

The Schiff base ligands and their corresponding metal complexes were successfully synthesized and characterized using spectral and elemental analyses. The synthesized Zn(II) complexes are colored, non-hygroscopic, and stable at room temperature. They are soluble in DMF, DMSO, and acetonitrile, but insoluble in water. The obtained analytical data are in good agreement with the calculated values, confirming the proposed compositions. Furthermore, the results indicate that the metal-to-ligand stoichiometry in these complexes is 1:2.

FT-IR Spectroscopy

FT-IR spectroscopy is a valuable technique for identifying functional groups and elucidating the coordination behavior of ligands with metal ions, including chelation and denticity. The FT-IR spectra of the Schiff base ligands and their metal complexes were recorded at room temperature over the range of 4000–250 cm^{-1} using KBr pellets.

The Schiff base ligands HL_1 and HL_2 exhibited characteristic azomethine (C=N) stretching bands at 1622 cm^{-1}. Upon complexation, these bands shift by approximately 2-4 cm^{-1}, indicating the participation of the azomethine nitrogen in coordination with the metal ion [15]. A broad band observed at 3460 cm^{-1} for HL_1 and 3467 cm^{-1} for HL_2, assigned to the phenolic –OH group, disappears after complexation, confirming the formation of a metal–oxygen (M-O) bond via the phenolic oxygen [15]. Moreover, the C-O stretching bands appear at 1174 cm^{-1} for HL_1 and 1152 cm^{-1} for HL_2. In the metal complexes, these bands shift to slightly lower frequencies by 6-8 cm^{-1}, further supporting coordination through the phenolic oxygen atom [16]. New bands appearing in the regions 521-545 cm^{-1} and 436-465 cm^{-1} in the complexes are attributed to M-O and M-N stretching vibrations, respectively [16]. A broad band observed at 3426 and 3452 cm^{-1} in complexes 1a and 2a indicates the presence of coordinated water molecules [15].

These spectral features clearly demonstrate that the ligands coordinate to the metal ions in a bidentate manner through both azomethine nitrogen and phenolic oxygen atoms, as illustrated in **Figures S1.1a** and **S1.2a.**

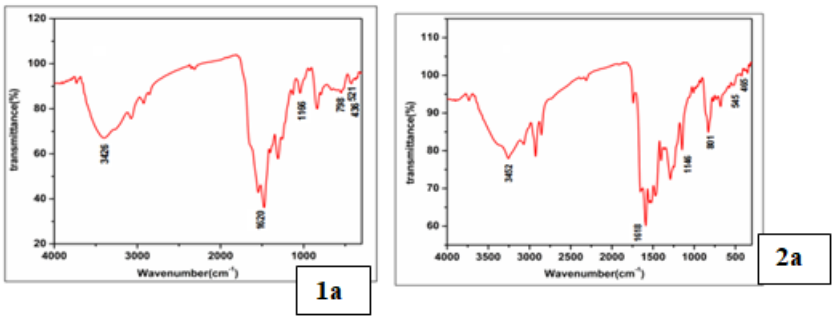

Fig. S1. FTIR spectrum of metal complexes 1a, and 2a in the region of 4000-250

COMPOUND	$\vartheta(O\text{-}H)$**cm^{-1}**	$\vartheta(C{=}N)$**cm^{-1}**	$\vartheta(C\text{-}O)$**cm^{-1}**	$\vartheta(M\text{-}O)$**cm^{-1}**	$\vartheta(M\text{-}N)$**cm^{-1}**
HL1	3460	1622	1174		
HL2	3467	1622	1152		
1a	3426(798)	1620	1166	521	436
2a	3452(801)	1618	1146	545	465

Table: 1. some notable IR frequencies (cm^{-1}) of Schiff base ligand and its metal complexes.

Electronic Spectra and Magnetic Moments

The electronic spectra of the synthesized Schiff base ligands HL1 and HL2 and their corresponding metal complexes (1a and 1b) were measured at room temperature using DMSO as the solvent. The spectral data are summarized in Table 2 and depicted in **Figures S2.1a** and **S2.1b**.

The free Schiff base ligands display two prominent absorption bands in the regions 260–258 nm (3846–3773 cm^{-1}) and 318–334 nm (3144–2994 cm^{-1}), which are assigned to π→π transitions within the aromatic rings and n→π* transitions of the azomethine (C=N) group, respectively [17]. In the metal complexes, these bands shifted to 254–265 nm (3937–3773 cm^{-1}) and 302–331 nm (3030–3211 cm^{-1}), indicating coordination between the ligand and the metal ions [15]. Furthermore, an additional absorption band emerges in the region 421–430 nm (2375–2325 cm^{-1}) in the metal complexes 1a and 1b respectively, which is absent in the free ligands. This band is attributed to ligand-to-metal charge transfer (LMCT) transitions [16]. Owing to the d^{10} electronic configuration of Zn(II), d–d transitions are not observed in its complexes. The effective magnetic moments of complexes 1a and 2a are found to be zero, confirming their diamagnetic nature. Overall, these spectral characteristics support the successful coordination of the Schiff base ligands with the metal ions.

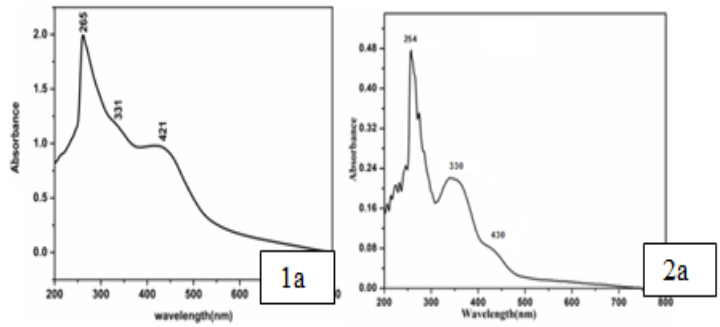

Fig. S2. UV-Vis spectra of spectrum of metal complexes 1a, and 2a in the region of 200-800nm.

ISSN No. 2454-6194 | DOI: 10.51584/IJRIAS |Volume XI Issue IX September 2026

COMPOUND	π-π*	n–π*	CT bands	μ_{effect}
HL1	260 (38461 cm^{-1})	318(31446 cm^{-1})		
HL2	258 (37736 cm^{-1})	334 (29940 cm^{-1})		
1a	265 (37736 cm^{-1})	331(30211 cm^{-1})	421(23753 cm^{-1})	0
2a	254 (39370 cm^{-1})	330 (30303 cm^{-1})	430 (23255 cm^{-1})	0

Table: 2. magnetic momentum and electronic spectra of schiff base and its metal complexes 1a, 1b and 1c.

ESI Mass Spectral Studies:

ESI mass spectrometry provides useful information about the molecular structure of a compound. The mass spectra of the metal complexes 1a and 2a showed molecular ion peaks at m/z = 747 ($[M+2]^+$) for 1a and m/z = 836.11 ($[M+2]^+$) for 2a (Figures S3.1a and S3.2a). These peaks confirm the formation of metal complexes with a $[M(L)_2]$ composition. The mass spectral results, along with elemental analysis, support a 1:2 metal-to-ligand ratio in the complexes.

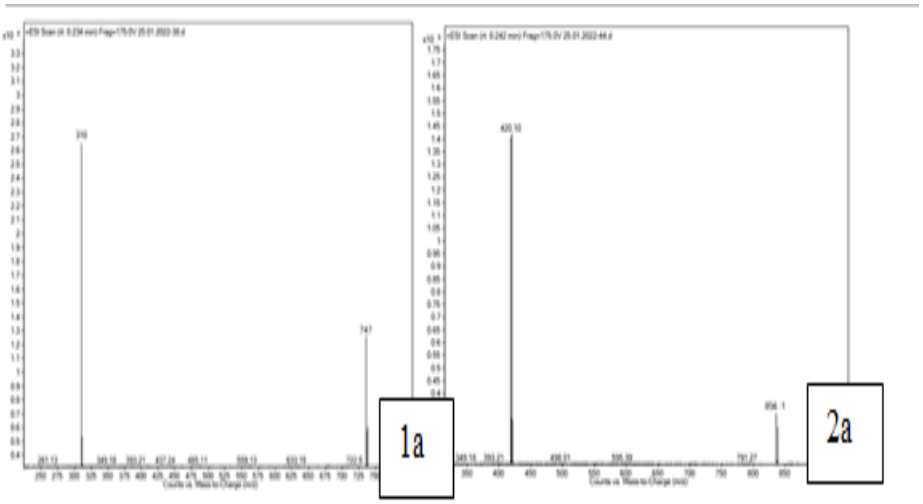

Fig. S3. ESI- Mass spectrum (positive ion mode) of the metal complexes 1a, and 2a.

Thermo gravimetric analysis:

Thermogravimetric analysis revealed that the two complexes (1a &2a) followed thermal decomposition pattern in two stages, as illustrated in **Figure S4**. Complex **1a** remained thermally stable up to 140 °C and then underwent an initial rapid decomposition between 140–180 °C, which can be attributed to the decomposition of two coordinated water molecules. The subsequent stage, characterized by a gradual weight loss from 285 to 585 °C, corresponds to the complete degradation of the organic framework, ultimately yielding a metal oxide residue [29]. In the case of complex **1b**, thermal stability was observed up to 155 °C. The first decomposition stage occurred between 155–179 °C, involving a rapid mass loss due to the removal of two water molecules. The second stage extended from 220 to 810 °C and involved a continuous weight loss, indicating the breakdown of the organic moiety and leading to the formation of the corresponding metal oxide residue.

Based on the combined interpretation of spectral studies and analytical data, the structures of the complexes are proposed as $[Zn(HL_1)_2(H_2O)_2]$ for complex **1a** and $[Zn(HL_2)_2(H_2O)_2]$ for complex **1b (Scheme I).**

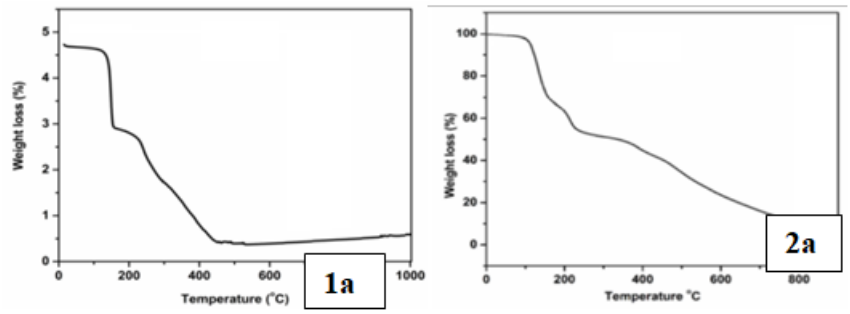

Fig.S4. TGA curve of complex 1a, and 2a

DNA binding studies:

Electronic absorption study:

In the current study, the interactions between CT-DNA and the metal complexes 1a and 2a were examined, and the changes in absorbance with and without CT-DNA are shown in Figure 4. Complexes **1a** and **2a** displayed absorption bands in the range of 254 and 265 nm, attributed to intra-ligand π–π* transitions. Upon the addition of CT-DNA, a decrease in absorbance (hypochromism) along with a slight red shift (bathochromic shift) was observed, suggesting that the metal complexes interact with DNA through an intercalation mode [19]. To estimate the intrinsic binding constant (Kb) of the complexes with CT-DNA, the equation $[DNA]/(\varepsilon_a-\varepsilon_f) = [DNA]/(\varepsilon_b-\varepsilon_f)+1/K_b(\varepsilon_b-\varepsilon_f)$ was used. In this equation, [DNA] is the concentration of CT-DNA (in base pairs), Kb is the intrinsic binding constant, εa is the apparent molar absorptivity (A_{obsd}/[complex]), and εf and εb are the molar extinction coefficients of the free and bound forms of the complex, respectively. The calculated binding constants were $1.365 \pm 0.02 \times 10^5$ M^{-1} for complex 1a and $3.421 \pm 0.02 \times 10^5$ M^{-1} for complex 2a [17,19]. These findings confirm that both complexes have a strong binding affinity for CT-DNA, with complex 2a showing greater binding strength than complex 1a. (For comparison, ethidium bromide has a K_b of 7×10^7 M^{-1}).

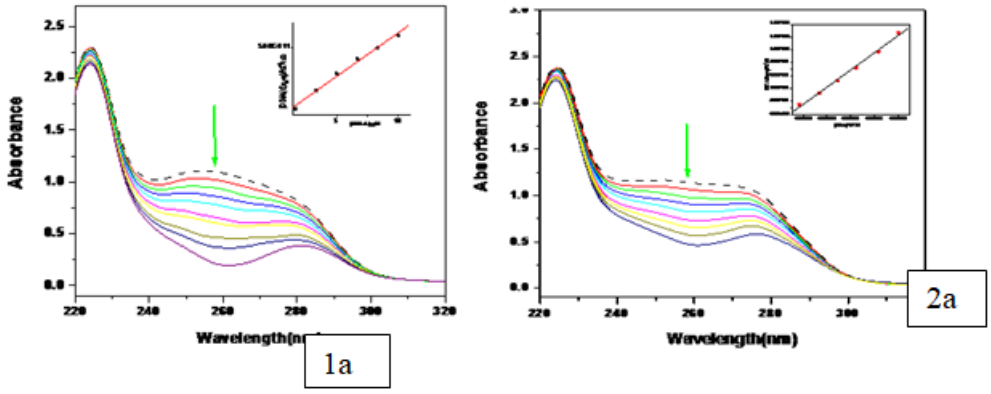

Fig. S5. UV-Vis absorption spectra of complexes 1a and 2a in Tris-HCl buffer (pH 7.2) at 25 °C in the presence (solid line) and absence (dashed line) of an increase in concentration of CT-DNA. For the determination of the intrinsic binding constant, Kb, for DNA binding, see the inset linear plot.

Fluorescence quenching study:

Fluorescence analysis using the emission intensity of the probe ethidium bromide (EB) was used to study the binding strength of metal complexes **1a** and **2a** with CT-DNA. In Tris-HCl buffer, EB shows weak fluorescence. When EB binds to CT-DNA by inserting between DNA base pairs (intercalation), its fluorescence intensity increases significantly [18,19]. However, adding metal complexes to the EB-DNA system reduces this fluorescence, suggesting that the complexes compete with EB for DNA binding through an intercalative mode [19], as shown in Figure 4. The strongest emission of EB-DNA is observed between 590–592 nm. The Stern–Volmer quenching constants (Ksv), obtained from fluorescence quenching data, revealed that complex 2a has a higher binding affinity than 1a. The Ksv values were $9.1 \pm 0.02 \times 10^3$ M^{-1} for 1a and $1.12 \pm 0.02 \times 10^4$ M^{-1} for

ISSN No. 2454-6194 | DOI: 10.51584/IJRIAS |Volume XI Issue IX September 2026

2a. Figure 5 shows the emission spectra of EB bound to CT-DNA in the absence and presence of the metal complexes **1a** and **2a (Fig. S6)**.

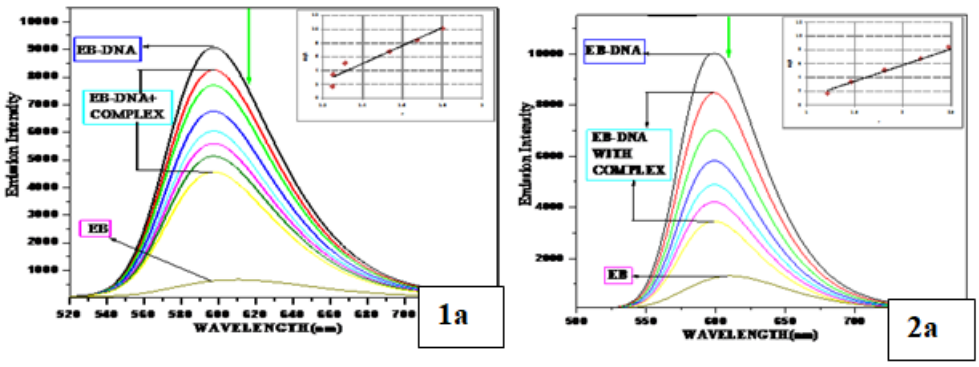

Fig. S6. shows the fluorescence emission spectra of the CT-DNA-EB system at 25 °C with and without an increase in the concentration of the complexes 1a, and 2a in Tris HCl buffer (pH 7.2). When the concentration of the complexes grew, the emission intensity decreased, as seen by the arrow (↓). Io/I vs r inset.

DNA cleavage activity:

The interaction of pBR322 DNA with the newly synthesized Schiff base ligands HL_1 and HL_2, along with their metal complexes **1a** and **2a**, was studied using gel electrophoresis under oxidative (with hydrogen peroxide) and photolytic (with UV light) conditions. DNA cleavage ability was assessed by tracking the transformation of supercoiled circular DNA (Form I) into nicked (Form II) and linear (Form III) forms. **Figures S.7.a and S.7.b** show the different DNA cleavage patterns observed during oxidative and photolytic treatments with HL_1, HL^2, and their metal complexes 1a and 2a. In the oxidative method **(Figure 7a)**, the DNA control, DNA with H_2O_2, and ligands HL_1 and HL^2 (lanes 1–4) did not cause any noticeable DNA cleavage. In contrast, lanes 5 and 6, containing complexes 1a and 2a, showed effective conversion of supercoiled DNA (Form I) into the nicked form (Form II). Similarly, in the photolytic method (Figure 7b), the DNA control and both ligands (lanes 1–3) showed no cleavage. However, the presence of metal complexes in lanes 4 (1a) and 5 (2a) resulted in clear DNA strand scission, converting Form I into Form II [20].

These findings indicate that the metal complexes exhibit stronger DNA cleavage activity than the free ligands. This enhanced activity could be due to electron transfer from the donor atoms in the ligands to the positively charged metal ion, which may increase the lipophilicity of the complexes and improve their interaction with DNA [21].

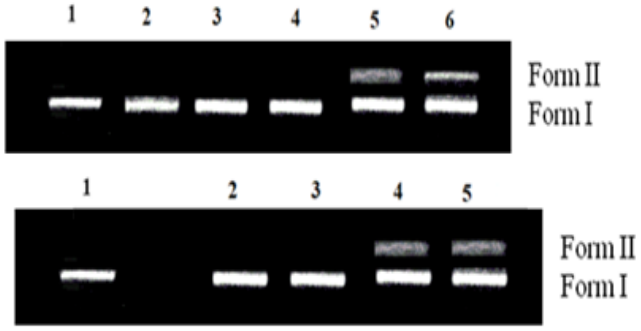

Figure. S7.(a). The metal complexes oxidatively cleaved supercoiled pBR322 DNA (0.2 µg, 33.3 µM) at 37 °C in a buffer of 5 mM Tris HCl/5 mM NaCl. 1st lane, DNA control: 2nd lane, DNA + H_2O_2 (1 mM); 3rd lane, DNA + H_2O_2 (1 mM) + HL_1; 4th lane, contains DNA + H_2O_2+HL_2; 5th lane contains DNA + H_2O_2 (1 mM) + 1a; 6th lane, contains DNA + H_2O_2 (1 mM) + 2a.Figure. S7.(b). Photoactivated cleavage of supercoiled pBR322 DNA by the complexes UV-light at 37 °C in 5 mM Tris HCl/5 mM NaCl buffer (long UV-365 nm). 1st lane, DNA control; 2nd lane, DNA + HL_1; 3rd lane, DNA + HL_2; 4th lane, DNA + 1a; 5th lane, DNA + 2a.

ISSN No. 2454-6194 | DOI: 10.51584/IJRIAS |Volume XI Issue IX September 2026

Biological studies:

Anti bacterial activity:

The antibacterial activity of the synthesized Schiff base ligands HL_1 and HL_2, along with their corresponding metal complexes 1a and 2a, was evaluated using the agar well diffusion method. As shown in **Table 3** and **Figure S8**, the metal complexes exhibited significantly higher antibacterial efficacy than their respective free ligands. This enhancement can be attributed to the chelation theory proposed by Tweedy, which suggests that metal coordination increases the biological activity of ligands. Among the tested compounds, complex 2a demonstrated the most potent inhibitory effect against both Gram-positive and Gram-negative bacterial strains, although its activity was lower than that of the standard drug.

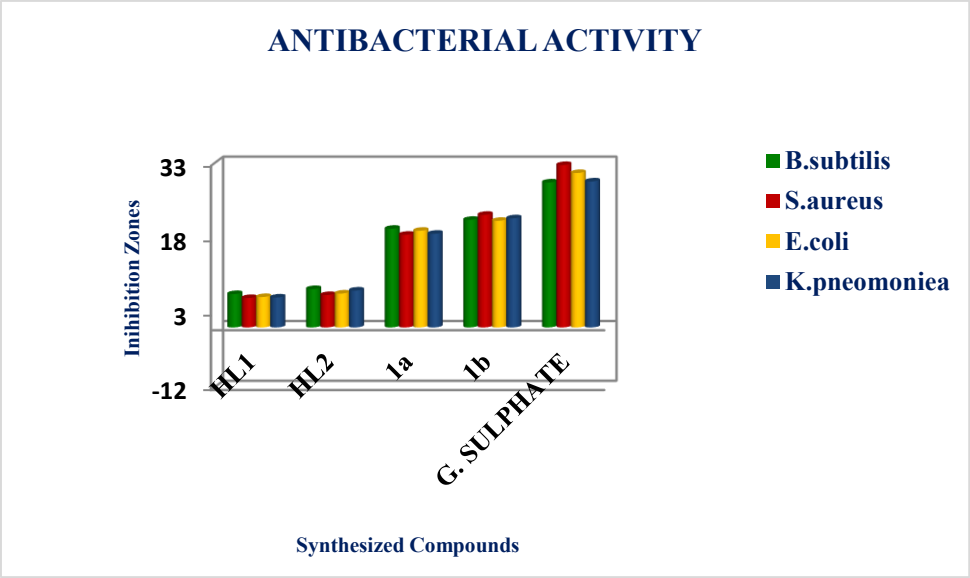

Fig. S8. Graphical representation of the antibacterial activity of Schiff bases (HL_1& HL_2) and their metal complexes (1a & 2a)

COMPOUND	GRAM POSITIVE BACTERIUM		GRAM NEGATIVE BACTERIUM	
	B.subtilis	S.aureus	E.coli	K.pneomoniea
HL_1	6.7	5.9	6.1	6
HL_2	7.7	6.5	6.8	7.4
1a	19.8	18.6	19.4	18.8
2a	21.6	22.6	21.4	21.9
GENTAMYCIN SULPHATE	29.1	32.6	31	29.3

Table: 3. Schiff base and metal complex antibacterial activity as inhibition zone diameters (mm) at 100 µg/ml concentration.

Antifungal activity:

The synthesized Schiff base HL_1 nd HL_2 and their metal complexes (1a and 2a) were evaluated for their in vitro antifungal efficacy against two fungal strains, Aspergillus niger and Candida albicans. Their performance was benchmarked against the well-established antifungal agent nystatin at an equivalent concentration (see **Table 4**

ISSN No. 2454-6194 | DOI: 10.51584/IJRIAS |Volume XI Issue IX September 2026

and Figure S.9). The results indicated that the metal complexes displayed enhanced antifungal activity relative to the free Schiff base ligand. Among them, complex 2a demonstrated notably stronger antifungal effects than complex 1a. This increased activity may be ascribed to the presence of an additional methyl group in the Schiff base ligand of complex 2a. However, it is important to note that the antifungal activity of these metal complexes remained lower than that of the standard drug, nystatin.

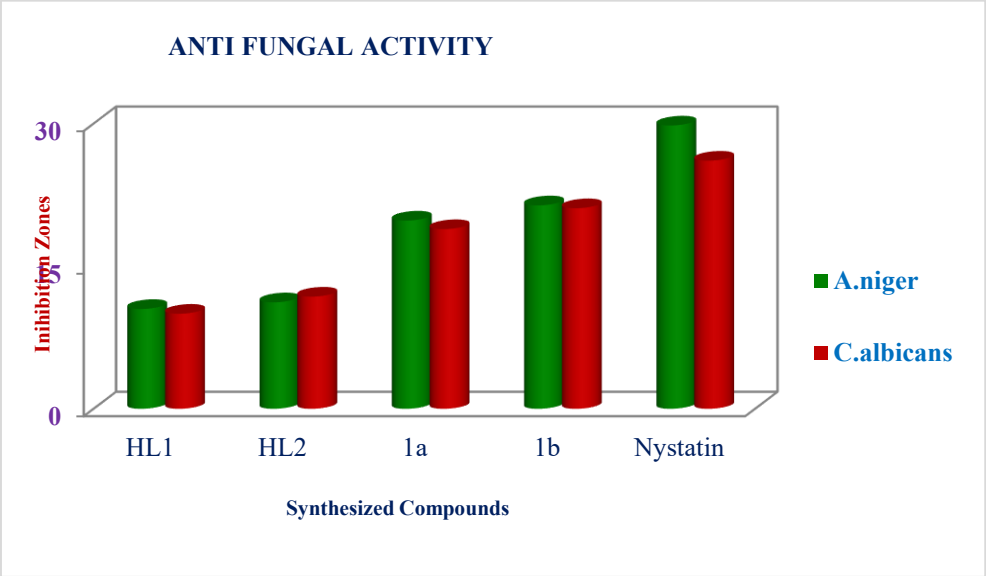

Fig. S9. Graphical representation of anti-fungal activity of Schiff bases (HL_1 & HL_2) and their metal complexes (1a & 2a)

COMPOUND	A.niger	C.albicans
HL_1	10.5	10
HL_2	11.2	11.8
1a	19.8	18.9
1b	21.4	21.1
Nystatin	29.8	26.1

Table: 4. Sciffs base and metal complex antifungal activity as inhibition zone diameters (mm) at 100 µg/ml concentration.

Anticancer activity (MTT assay):

The anticancer activity of the Schiff base ligands HL_1 and HL_2, along with their metal complexes 1a and 2a, was assessed using the MTT assay against MCF-7 (human breast cancer) and A-549 (human lung adenocarcinoma) cell lines. Doxorubicin, a well-established anticancer drug, served as the reference standard. The IC_{50} values of all synthesized compounds are presented in **Table 5** and**Figure S.10**. The cytotoxicity data indicated that all tested complexes exhibited significant cytotoxic effects against the MCF-7 cell line, surpassing their activity against the A-549 cell line. Among them, complex 2a exhibited the most pronounced cytotoxicity. Moreover, all metal complexes demonstrated enhanced activity compared to their corresponding free ligands, suggesting that metal coordination improved the anticancer potential of the compounds. The order of cytotoxicity was found to be $HL_1 < HL_2 < 1a < 2a$.

ISSN No. 2454-6194 | DOI: 10.51584/IJRIAS |Volume XI Issue IX September 2026

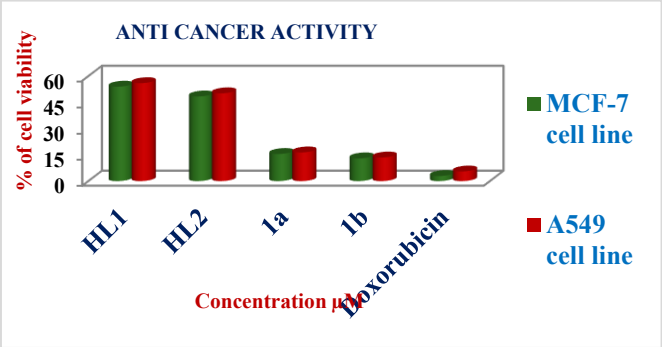

Fig.S10. anticancer activity of Schiff bases (HL_1& HL_2) and their metal complexes (1a & 2a) against MCF-7 and A549 cell lines.

Compound	IC_{50}(MCF-7)	IC_{50}(A549)
HL_1	54	56
HL_2	48.4	50.2
1a	15.5	16.4
2a	13	13.5
Doxorubicin	2.9	5.5

Table:5. Anticancer activity of schiff base and its metal complexes against MCF-7 (human breast cancer cell line) and A-549 (human lung adenocarcinoma cell line).

CONCLUSION

Three novel Schiff base metal complexes 1a and 2a have been synthesized from a Schiff base ligands HL_1 and HL_2, which is characterized by elemental analysis and spectral analysis such as FT-IR, UV-Vis, Mass, and TGA, which revealed that the Zn(II) complexes exhibited an octahedral geometry, coordination water molecule is present in the Zn(II) complexes which were confirmed by FT-IR and TGA. DNA interaction studies revealed that two synthesized complexes bind via intercalative mode. DNA interaction studies concluded that the synthesized three complexes cleaved into nicked or linear form in both cleavage modes. Biological studies performed by antimicrobial, and cytotoxicity have shown that the 2a complex have shown enhanced activity compared to a complex and their respective ligands.

ACKNOWLEDGEMENTS

We would like to express our sincere thanks to the Head, Department of Chemistry for providing the necessary facilities for carrying out the work successfully. We are thankful to Director, CFRD, Osmania University and the Director, NITW for providing spectral and analytical data.

REFERENCES

1. McQuitty, R.J. Metal-based drugs. Sci. Prog. 2014, 97, 1–19. [CrossRef] [PubMed]
2. Sodhi, R.K. Metal Complexes in Medicine: An Overview and Update from Drug Design Perspective. Cancer Ther. Oncol. Int. J. 2019, 14.
3. Gali Ramesh,Sreenu Daravath,M Swathi,V. Sumalatha,Dasari Shiva Shankar,Shivaraj. Investigation on Co(II), Ni(II), Cu(II) and Zn(II) complexes derived from quadridentate salen-type Schiff base: Structural characterization, DNA interactions, antioxidant proficiency and biological evaluation. Chemical Data Collections. 28(2020) 100434.

4. Liu, X.; Hamon, J.R. Recent developments in penta-, hexa- and heptadentate Schiff base ligands and their metal complexes. Coord. Chem. Rev. 2019, 389, 94–118.
5. Sarker, D.; Karim, M. R.; Haque, M. M.; Zamir, R.; Asraf, M. A., Copper (II) Complex of Salicylaldehyde Semicarbazone: Synthesis, Characterization and Antibacterial Activity. Asian Journal of Chemical Sciences.2019, 1-8.
6. Sarker, D.; Reza, M. Y.; Haque, M. M.; Zamir, R.; Asraf, M. A., Synthesis, Characterization, Antibacterial and Thermal Studies of Cu (II) Complex of Thiophene-2-aldehyde Semicarbazone. Asian Journal of Applied Chemistry Research.2019, 1-10.
7. Ndagi, U.; Mhlongo, N.; Soliman, M.E. Metal complexes in cancer therapy - an update from drug design perspective. Drug design, development and therapy 2017, 11, 599-616,
8. Shahabadi, N.; Mohammadi, S. Synthesis Characterization and DNA Interaction Studies of a New Zn(II) Complex Containing Different Dinitrogen Aromatic Ligands. Bioinorganic Chemistry and Applications 2012, 2012, 1-8,
9. Bastaki A, Inter J Diabetes Metab, 13 (2005) 111.
10. Whitcomb D C & Lowe M E, Dig Dis Sci, 52 (2007) 1.
11. A. A. Maihub, U. K. Mahanta, G. Badhei, R. K. Mohapatra, P. K. Das, Rasayan J. Chem. 2018, 11, 166.
12. R.W.Y. Sun, C.M. Che, The anti-cancer properties of gold(III) compounds with dianionic porphyrin and tetradentate ligands, Coord. Chem. Rev. 253 (2009) 1682–1691.
13. Sreenu Daravath, Marri Pradeep Kumar, Aveli Rambabu, Narendrula Vamsikrishna, Nirmala Ganji, Shivaraj. Design, synthesis, spectral characterization, DNA interaction and biological activity studies of copper(II), cobalt(II) and nickel(II) complexes of 6-amino benzothiazole derivatives. Journal of Molecular Structure.Volume 1144, 15 (2017) 147-158.
14. K. Jagadesh Babu, Sreenu Daravath,M. Swathi, Dasari Ayodhya, Shivaraj. Synthesis, anticancer, antibacterial, antifungal, DNA interactions, ADMET, molecular docking, and antioxidant evaluation of novel Schiff base and their Co(II), Ni(II) and Cu(II) complexes. Res Chem, 6 (2023) 101121.
15. K Jagadesh babu, Synthesis, Spectroscopic Characterization, DNA Binding, and Biological Evaluation of Zn(II) Complexes Derived from 5-Cyclohexylanisidine-Based Schiff Bases, Volume - 11, 62 (2025) 194-205.
16. Babu, K.J., Ayodhya, D., Shankar, D.S. et al. Multifaceted evaluation of novel Co(II), Ni(II), and Cu(II) metal complexes: a promising approach for DNA interaction, antimicrobial, antioxidant, anticancer, and ADME studies. J IRAN CHEM SOC 23, 276 (2026). https://doi.org/10.1007/s13738-026-03543-6
17. K Jagadesh babu, Koyada Vivek. Design, synthesis, and biological evaluation of novel 6-aminobenzothiazole -based zink (Ii) metal complexes with anticancer, antimicrobial, adme applications and dna-binding studies. International Journal of Chemical Science 10(2026)2:95-105 DOI:10.66856/chemical.2026.10.2.10033.
18. Gali Ramesh, Sreenu Daravath, K. Jagadesh Babu1,Ravinder Dharavath, Amit Ranjan, Dasari Ayodhy, Shivaraj. Design, Synthesis, Structural Investigation and Photo Induced Biological Investigations of Co(II), Ni(II) and Cu(II) Complexes Derived from N,O Donor Schiff Bases. J. Flu 34 (2024) 2087–2108.
19. N. Jyothi, Sreenu Daravath, M. Swathi, K Jagadeshbabu, Nirmala Ganji, Shivaraj. Synthesis, geometry optimization and non-isothermal kinetic parameters of copper(II), nickel(II) and cobalt(II) complexes of 5-(trifluoromethyl)-2-methoxybenzenamine: DNA binding, cytotoxicity, antioxidant and antimicrobial activity. J Mol Stru 1295, 1(2024) 136529.
20. K. Jagadesh Babu, Dasari Ayodhyaa, Shivaraj. Comprehensive investigation of Co(II), Ni(II) and Cu(II) complexes derived from a novel Schiff base: Synthesis, characterization, DNA interactions, ADME profiling, molecular docking, and in-vitro biological evaluation.Results in Chemistry.6[2023]101110.https://doi.org/10.1016/j.rechem.2023.101110.